A hyperboloidal method for numerical simulations of multidimensional nonlinear wave equations

Oliver Rinne

HTW Berlin - University of Applied Sciences

Virtual Infinity Seminar
Hyperboloidal Research Network

19 September 2025

https://arxiv.org/abs/2507.00674

Outline

Outline of the talk

Nonlinear wave equation (NLW)

$$\Box\Phi := -\partial_t^2\Phi + \Delta\Phi = \mu|\Phi|^{p-1}\Phi, \quad \Phi : \mathbb{R}\times\mathbb{R}^n \to \mathbb{R}, \quad p > 1,$$

$\mu = -1$ focusing, $\mu = 1$ defocusing

- Model for nonlinear wavelike equations in fluid dynamics, optics, acoustics, plasma physics, GR, QFT, ...
- Related equations: nonlinear Schrödinger, Korteweg–de Vries, Klein–Gordon, Yang–Mills, wave map, ...
- Rich behaviour of solutions due to interplay between dispersion and nonlinearity
- In general, small initial data will scatter, large initial data will cause blow-up (in the focusing case at least)
- In some cases stable regular soliton solutions exist, which may prevent solutions from scattering
- Much recent interest in analysing global well posedness [Bourgain 1999, Kenig & Merle 2008, Dodson 2016, ...]

Energy criticality

- NLW is invariant under the rescaling

$$\Phi(t,x) \to \lambda^{\frac{2}{p-1}} \Phi(\lambda t, \lambda x)$$

- Conserved energy ($\partial_t E = 0$)

$$E(\Phi, \partial_t \Phi) = \int_{\mathbb{R}^n} \left(\tfrac{1}{2}(\partial_t \Phi)^2 + \tfrac{1}{2}\|\nabla \Phi\|^2 + \tfrac{\mu}{p+1}|\Phi|^{p+1} \right) \mathrm{d}x$$

- Energy is invariant under the rescaling iff the NLW is (energy-)critical,

$$p = \frac{n+2}{n-2} =: p_{\text{crit}}$$

- $p < p_{\text{crit}}$ subcritical, $p > p_{\text{crit}}$ supercritical

Unbounded domains: truncation

- How do we deal numerically with the infinite spatial domain?

- Simplest approach: truncate, radius $r \leqslant R$ with R suitably large
- Boundary conditions at $r = R$ are needed in order to obtain a well-posed initial-boundary value problem.
- Exact absorbing (a.k.a. transparent, non-reflecting, radiative) boundary conditions are not known in the nonlinear case.
- Naive boundary conditions (e.g. Dirichlet) will generally cause spurious reflections.
- Moreover, we cannot determine the solution for $r > R$.

Spatial compactification

- Compactify radius, e.g.

$$r = \frac{2a\tilde{r}}{1-\tilde{r}^2}, \quad \tilde{r} \in (0,1), \quad a = \text{const} \ \ (=6 \text{ in plots below})$$

- Characteristics of the NLW:

$$t \pm r = \text{const},$$

  $+$ ingoing (red),
  $-$ outgoing (blue)

- In $(t, \tilde{r})$ coordinates, outgoing characteristics pile up near $\tilde{r} = 1$.
- Waves ultimately fail to be resolved numerically as they travel outwards.

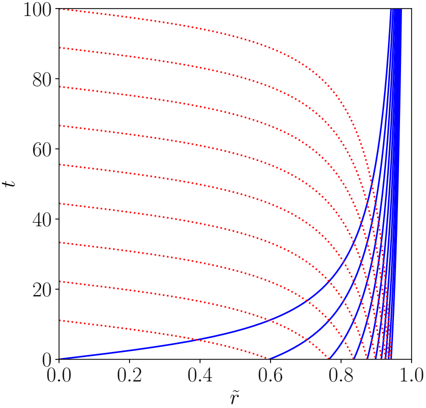

Hyperboloidal compactification

- Introduce a new time coordinate

$$\tilde{t} = t - \sqrt{a^2 + r^2}$$

- Outgoing characteristics smoothly leave the domain.
- No incoming characteristics $\Rightarrow$ no boundary conditions needed at future null infinity $\mathscr{I}^+$ ($\tilde{r} = 1$).
- Radiation can be read off there.

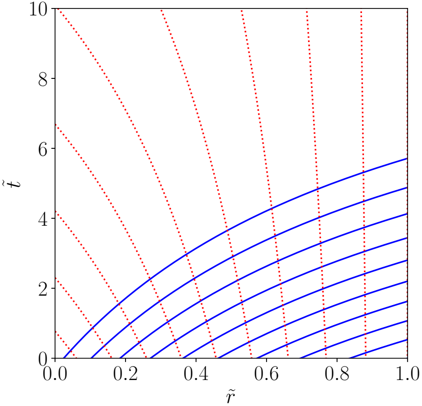

Hyperboloidal slices

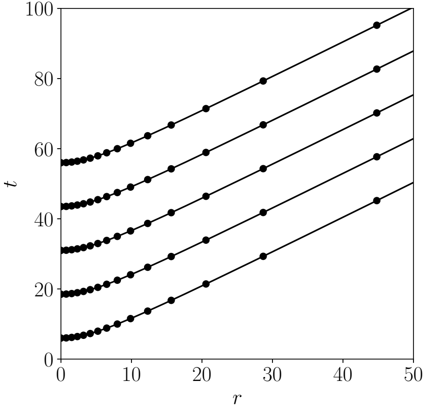

A few hyperboloidal slices in the (r, t) plane (evenly spaced in $\tilde{t}$) and a numerical grid that is uniform in $\tilde{r}$

Polar coordinates, symmetry assumptions

- We use spherical polar coordinates

$$r \in (0, \infty), \quad \theta_1, \ldots, \theta_{n-2} \in [0, \pi], \quad \varphi \in [0, 2\pi)$$

- Most previous numerical work has assumed radial symmetry [Strauss & Vazquez 1978, …].
- Exceptions: [Zenginoğlu & Kidder 2010/11] evolve cubic ($p = 3$) NLW in $n = 3$ without symmetries.
- Here we do not assume any symmetries for $n = 3$.
- For $n > 3$ we impose $\mathrm{SO}(n-1)$ symmetry so there is one effective angular coordinate θ on the sphere.
- Let $\sigma^{(n-1)}$ denote the standard metric on the sphere S^{n-1} and $\mathring{\Delta}^{(n-1)}$ its Laplace–Beltrami operator.
- Under $\mathrm{SO}(n-1)$ symmetry,

$$\mathring{\Delta}^{(n-1)} = \partial_\theta^2 + (n-2) \cot\theta \, \partial_\theta$$

Outline of the talk

Hyperboloidal foliation of Minkowski spacetime

- $(n+1)$-dimensional Minkowski metric

$$\eta = -\mathrm{d}t^2 + \mathrm{d}r^2 + r^2\sigma^{(n-1)}$$

- Introduce a new time coordinate

$$\tilde{t} = t - \sqrt{a^2 + r^2}, \quad a = \frac{n}{C} > 0$$

- Hypersurfaces $\tilde{t} = \mathrm{const}$ are hyperboloids, C is their constant mean curvature (taken to be $C = 0.5$ in the numerical evolutions).
- Also introduce a compactified radius $\tilde{r}$:

$$r = \frac{2n\tilde{r}}{C(1-\tilde{r}^2)}$$

Conformal metric

- Minkowski metric in the new coordinates takes the form

$$\eta = \Omega^{-2} \left[-\tilde{\alpha}^2 \mathrm{d}\tilde{t}^2 + (\mathrm{d}\tilde{r} + \tilde{\beta}^{\tilde{r}} \mathrm{d}\tilde{t})^2 + \tilde{r}^2 \sigma^{(n-1)} \right] =: \Omega^{-2} \tilde{\eta}$$

- Conformal factor $\Omega = \frac{\tilde{r}}{r} = \frac{C}{2n}(1 - \tilde{r}^2)$, conformal metric $\tilde{\eta}$
- Conformal lapse $\tilde{\alpha} = \frac{C}{2n}(1 + \tilde{r}^2)$ and shift $\tilde{\beta}^{\tilde{r}} = -\frac{\tilde{r}}{a} = -\frac{C}{n}\tilde{r}$
- $\tilde{r}$ has been chosen such that the spatial conformal metric is flat,

$$\tilde{\gamma} = \mathrm{d}\tilde{r}^2 + \tilde{r}^2 \sigma^{(n-1)}$$

- Scalar curvature (Ricci scalar) of η is $R = 0$ (flat)
  but for the conformal metric $\tilde{\eta}$,

$$\tilde{R} = \frac{4n[-\tilde{r}^4 + (n-5)\tilde{r}^2 + n]}{(\tilde{r}^2 + 1)^3}$$

Nonlinear wave equation

- Start with NLW

$$\Box\Phi = \mu|\Phi|^{p-1}\Phi$$

- Define a conformally rescaled scalar field

$$\tilde{\Phi} = \Omega^{(1-n)/2}\Phi$$

- Using the conformal identity

$$\tilde{\Box}\tilde{\Phi} - \frac{n-1}{4n}\tilde{R}\tilde{\Phi} = \Omega^{-(n+3)/2}\left(\Box\Phi - \frac{n-1}{4n}R\Phi\right)$$

and $R = 0$, we obtain

$$\tilde{\Box}\tilde{\Phi} - \frac{n-1}{4n}\tilde{R}\tilde{\Phi} = \mu\Omega^{[p(n-1)-n-3]/2}|\tilde{\Phi}|^{p-1}\tilde{\Phi}$$

Conformal 3+1 decomposition

- $\tilde{\nu} :=$ unit future-directed normal to $\tilde{t} = \text{const}$ slices
- Lie derivative $\mathcal{L}_{\tilde{\nu}}\tilde{\Phi} = \tilde{\alpha}^{-1}(\partial_{\tilde{t}} - \tilde{\beta}^{\tilde{r}}\partial_{\tilde{r}})\tilde{\Phi}$
- Conformal mean curvature of $\tilde{t} = \text{const}$ slices: $\tilde{K} = -\dfrac{2n}{\tilde{r}^2+1}$
- With these definitions the NLW reads

$$-\mathcal{L}_{\tilde{\nu}}^2\tilde{\Phi}+\tilde{\Delta}\tilde{\Phi}+\tilde{K}\mathcal{L}_{\tilde{\nu}}\tilde{\Phi}+\tilde{\alpha}^{-1}\tilde{\nabla}\tilde{\alpha}\cdot\tilde{\nabla}\tilde{\Phi}-\tfrac{n-1}{4n}\tilde{R}\tilde{\Phi} = \mu\Omega^{[p(n-1)-n-3]/2}|\tilde{\Phi}|^{p-1}\tilde{\Phi}$$

- Write in first-order form in time by introducing $\tilde{\Pi} := \mathcal{L}_{\tilde{\nu}}\tilde{\Phi}$:

$$\begin{aligned}
\tilde{\Phi}_{,\tilde{t}} &= \tilde{\beta}^{\tilde{r}}\tilde{\Phi}_{,\tilde{r}} + \tilde{\alpha}\tilde{\Pi},\\
\tilde{\Pi}_{,\tilde{t}} &= \tilde{r}^{1-n}\left[\tilde{r}^{n-1}\left(\tilde{\beta}^{\tilde{r}}\tilde{\Pi} + \tilde{\alpha}\tilde{\Phi}_{,\tilde{r}}\right)\right]_{,\tilde{r}} + \tilde{\alpha}\tilde{r}^{-2}\mathring{\Delta}^{(n-2)}\tilde{\Phi} - \frac{n-1}{4n}\tilde{\alpha}\tilde{R}\tilde{\Phi}\\
&\quad -\mu\tilde{\alpha}\Omega^{[p(n-1)-n-3]/2}|\tilde{\Phi}|^{p-1}\tilde{\Phi}
\end{aligned}$$

- Regular at $\mathscr{I}^+$ ($\tilde{r} = 1$) provided that

$$p \geqslant p_{\text{conf}} := \frac{n+3}{n-1} > p_{\text{crit}} \text{ for } n \geqslant 3$$

Energy balance

- Scalar field Φ is associated with energy-momentum tensor

$$T_{ab} = \nabla_a\Phi\nabla_b\Phi - \frac{1}{2}\eta_{ab}\nabla_c\Phi\nabla^c\Phi - \frac{\mu}{p+1}|\Phi|^{p+1}\eta_{ab},$$

  where ∇ is covariant derivative of Minkowski metric η
- Conservation of energy and momentum: $\nabla^b T_{ab} = 0$
- Killing vector (symmetry) $k = \partial_t$ gives rise to conserved current

$$E^a = T^a{}_b k^b = T^a{}_t, \qquad \nabla_a E^a = 0$$

- Applying Gauss' law yields energy balance of the form

$$E(\tilde{t}_2) - E(\tilde{t}_1) = F(\tilde{t}_1, \tilde{t}_2),$$

  where $E(\tilde{t})$ is energy on hyperboloidal slice of constant time $\tilde{t}$ and $F(\tilde{t}_1, \tilde{t}_2)$ is integrated energy flux at $\mathscr{I}^+$ between $\tilde{t}_1$ and $\tilde{t}_2$

Energy balance

- Here the energy is

$$
\begin{aligned}
E(\tilde{t}) \;=\; & \frac{C}{4n}\int_0^1 \tilde{r}^{n-1}\mathrm{d}\tilde{r}\int_{S^{n-1}} dS^{(n-1)}\Big\{(1+\tilde{r}^2)\Big[\tilde{\Pi}^2+\tilde{\Phi}_{,\tilde{r}}^2 \\
& +\frac{1}{\tilde{r}^2}\|\mathring{\tilde{\nabla}}^{(n-1)}\tilde{\Phi}\|^2 + 2\mu\Omega^{[p(n-1)-n-3]/2}\frac{1}{p+1}|\tilde{\Phi}|^{p+1}\Big] \\
& +2(n-1)\frac{\tilde{r}^2-1}{\tilde{r}^2+1}\,\tilde{r}\tilde{\Phi}_{,\tilde{r}}\tilde{\Phi} - 4r\tilde{\Phi}_{,\tilde{r}}\tilde{\Pi} + (n-1)^2\frac{\tilde{r}^2}{\tilde{r}^2+1}\tilde{\Phi}^2\Big\}
\end{aligned}
$$

(highlighting the potential energy contribution)

- The flux is manifestly negative, showing that waves carry away energy at infinity:

$$
F(\tilde{t}_1,\tilde{t}_2) = -\frac{C^2}{n^2}\int_{\tilde{t}_1}^{\tilde{t}_2}\mathrm{d}\tilde{t}\int_{S^{(n-1)}} dS^{(n-1)}(\tilde{\Phi}_{,\tilde{r}}-\tilde{\Pi})^2\Big|_{\tilde{r}=1}
$$

Outline of the talk

Spatial discretisation: radial finite differences

- Introduce equidistant grid points, staggered about axis and origin

$$
\begin{aligned}
\tilde{r}_i &= (i + \tfrac{1}{2})h_{\tilde{r}}, \quad i = 0, 1, \dots, N_{\tilde{r}} - 1, \quad h_{\tilde{r}} = 1/(N_{\tilde{r}} - \tfrac{1}{2}),\\
\theta_j &= (j + \tfrac{1}{2})h_\theta, \quad j = 0, 1, \dots, N_\theta - 1, \quad h_\theta = \pi/N_\theta,\\
\varphi_k &= k h_\varphi, \quad k = 0, 1, \dots, N_\varphi - 1, \quad h_\varphi = 2\pi/N_\varphi
\end{aligned}
$$

- Discretise radial derivatives using centred fourth-order finite differences.
- One-sided finite differences near outer boundary $\tilde{r} = 1$
- Near the origin, fill values at ghost points $\tilde{r}_{-1}$ and $\tilde{r}_{-2}$ using

$$u(-\tilde{r}, \theta, \varphi) = u(\tilde{r}, \pi - \theta, \pi + \varphi)$$

Spatial discretisation: pseudospectral method

- Any smooth function on the sphere must obey

$$u(-\theta,\varphi) = u(\theta,\pi+\varphi), \qquad u(\pi+\theta,\varphi) = u(\pi-\theta,\pi+\varphi)$$

- Fourier expansion, here in $n = 3$ without symmetries:

$$u(\theta,\varphi) \approx \sum_{l=0}^{N_\theta-1} \left(\cos(l\theta) \sum_{\substack{m=0 \\ m \text{ even}}}^{N_\varphi/2-1} a_{lm}\, e^{im\varphi} + \sin(l\theta) \sum_{\substack{m=1 \\ m \text{ odd}}}^{N_\varphi/2-1} a_{lm}\, e^{im\varphi} \right)$$

- Transform between expansion coefficients a_{lm} and grid point values $u_{jk} := u(\theta_j,\varphi_k)$ using fast Fourier transform techniques
- Main object in the code is array of values of $\tilde{\Phi}$ and $\tilde{\Pi}$ at grid points $(\tilde{r}_i,\theta_j,\varphi_k)$.
- Nonlinear terms are evaluated pointwise.

Time stepping and filtering

- Method of lines: First discretise in space $\rightarrow$ system of ODEs
- Integrate forward in time using fourth-order Runge-Kutta method
- Add fifth-order dissipation [Kreiss-Oliger 1973] in radial direction to obtain stable finite-difference method (higher order than numerical truncation error)
- To avoid spectral aliasing, apply spectral filtering (2/3 rule)
- To alleviate clustering of grid points near the poles of the two-sphere, filter out proportion $1 - \sin\theta$ of all φ-Fourier modes
- Time step is restricted by smallest distance between neighbouring grid points:

$$\Delta\tilde{t} = \lambda \Delta x_{\text{min}}, \quad \Delta x_{\text{min}} = \tfrac{1}{2} h_{\tilde{r}} h_{\theta}$$

  with $0 < \lambda < 1$ [Courant–Friedrichs–Lewy], typically $\lambda = 0.8$
- Typical numerical resolution is $N_{\tilde{r}} = 4000$, $N_{\theta} = N_{\varphi} = 12$

Spatial integration

- Radial integration is performed using Simpson's rule (same order of numerical truncation error as finite-difference scheme, $\mathcal{O}(h_{\tilde{r}}^4)$).
- Fourier spectral expansion can be integrated directly:

$$\int_{S^2} u \, dS^{(2)} = \int_0^{2\pi} \int_0^{\pi} u(\theta, \varphi) \sin\theta \, \mathrm{d}\theta \, \mathrm{d}\varphi \approx 2\pi \sum_{\substack{l=0 \\ l \text{ even}}}^{N_\theta - 1} \frac{2 a_{l0}}{1 - l^2}$$

- Generalisation to higher dimensions is straightforward.

Outline of the talk

Convergence test against exact linear solutions

- We have constructed exact solutions to the *linear* wave equation in various dimensions, based on expansion in spherical harmonics $Y_{lm}(\theta, \varphi)$.
- Plot L^2 norm of error of numerical vs. exact solution
- Here $n = 3$, initial data containing two spherical harmonics $(l, m) = (1, 1)$ and $(2, -2)$

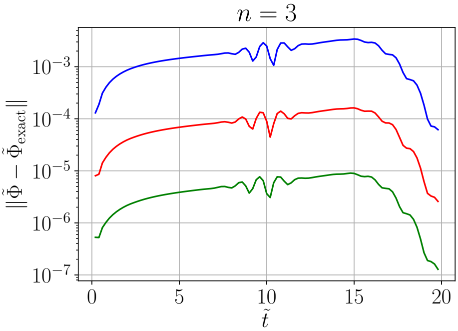

- $N_{\tilde{r}} = 250, 500, 1000$
- Approximate fourth-order convergence

Nonlinear evolution

- $n = 5$ under SO(4) symmetry, focusing, cubic nonlinearity ($p = 3$)
- Momentarily static initial data containing two spherical harmonics with $l = 1$ and $l = 2$

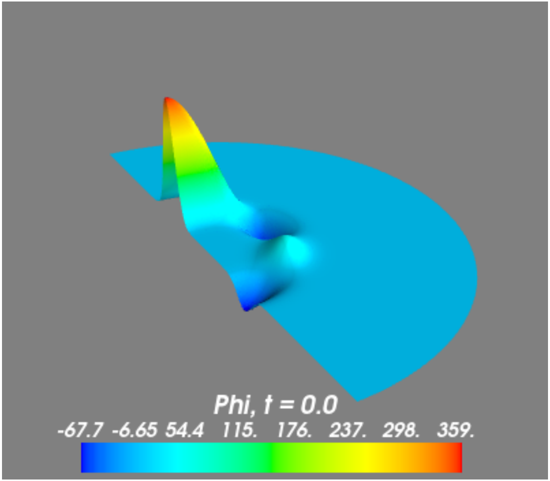

Energy balance: numerical conservation

- Numerically evaluated energy $E(\tilde{t})$, integrated flux $-F(0,\tilde{t})$ and their sum. Focusing (solid) vs. defocusing (dashed) NLW.
- Energy balance is well satisfied numerically:

$$E(\tilde{t}) - F(0,\tilde{t}) = E(0) = \text{const}$$

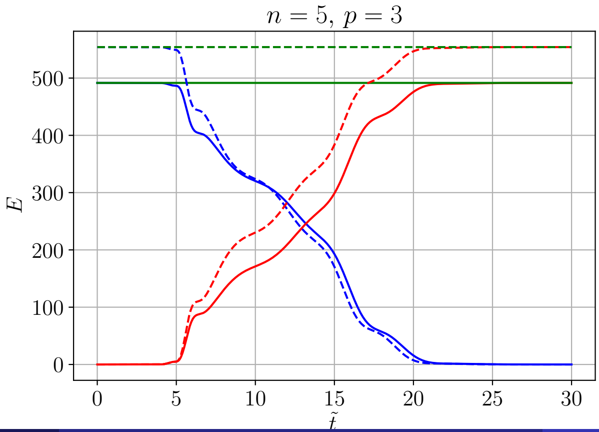

Energy balance: convergence

Relative error in violation of energy balance ($n = 5$, $p = 3$, defocusing).

left: varying radial resolution ($N_{\tilde{r}} = 1000, 2000, 4000$) at fixed $N_\theta = 24$,
right: varying angular resolution ($N_\theta = 16, 20, 24$) at fixed $N_{\tilde{r}} = 4000$.

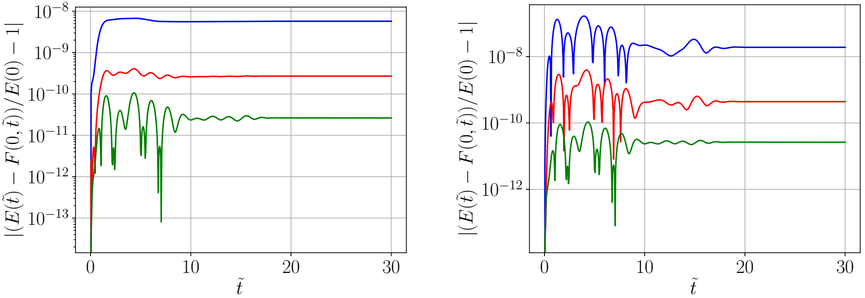

Potential energy contribution

- Ratio of potential energy and total energy, focusing (solid) vs. defocusing (dashed)
- Potential energy becomes negligible at late times.

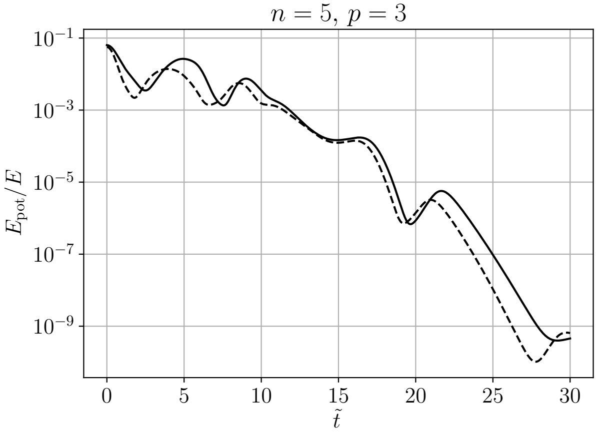

Tails

- Extract the scalar field at a fixed radius $\tilde{r}_{\text{ex}}$ and expand into (real basis of) spherical harmonics

$$\tilde{\Phi}|_{\tilde{r}=\tilde{r}_{\text{ex}}} = \sum_{l=0}^{\infty} \sum_{m=-l}^{l} \tilde{\Phi}_{lm}(\tilde{t})\, \hat{Y}_{lm}(\theta, \varphi)$$

- Each mode $\tilde{\Phi}_{lm}$ shows a power-law decay $\sim \tilde{t}^{-q_{lm}}$ at late times, the so-called tail.
- Compute the local power index

$$q_{lm}(\tilde{t}) := -\frac{\mathrm{d} \ln \tilde{\Phi}_{lm}}{\mathrm{d} \ln \tilde{t}}\Big|_{\tilde{r}=\tilde{r}_{\text{ex}}}$$

- This will approach a constant decay rate q_{lm} as $\tilde{t} \to \infty$.
- Observe that the decay rate is the same for focusing and defocusing NLW with the same exponent p of the nonlinearity.

Tails: azimuthal independence

- Evolution for $n = 3$, $p = 5$ below has initial data containing two spherical harmonics with $(l, m) = (2, 1)$ and $(2, 2)$.
- Find that q_{lm} is independent of m, hence focus on $SO(n-1)$ symmetry in the following.

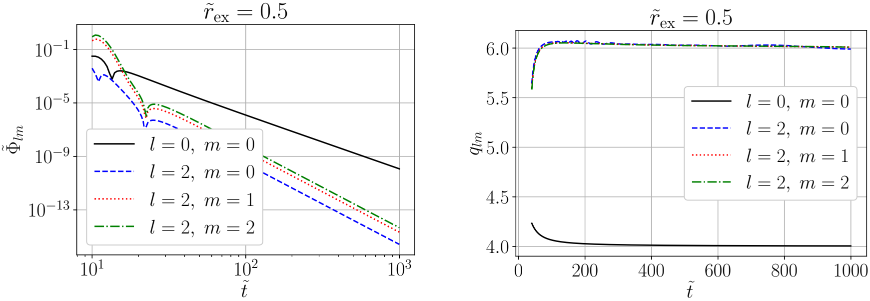

Tails: convergence (here $n = 3, p = 5$)

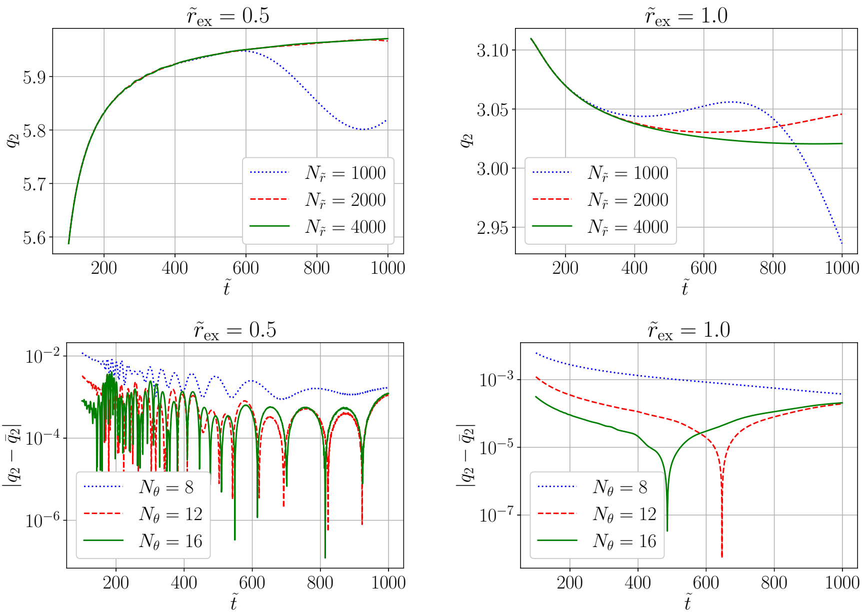

Tails: radial dependence

- Local power index $q_2(t)$ extracted at four different radii: $\tilde{r}_{ex} = 0.5$, 0.9, 0.99 and 1
- Same asymptotic decay rate at any finite radius but a slower decay rate at $\mathscr{I}^+$ ($\tilde{r} = 1$)

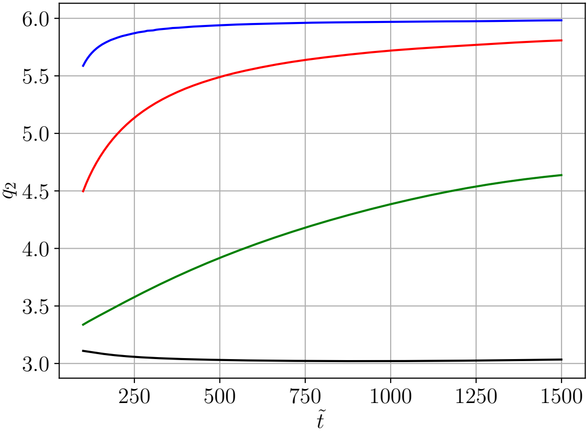

Tails: dependence on spherical harmonics

- Compare local power index q_2 at a finite radius and at $\mathscr{I}^+$ for $l = 0, 1, 2, 3$
- Here again $n = 3$, $p = 5$

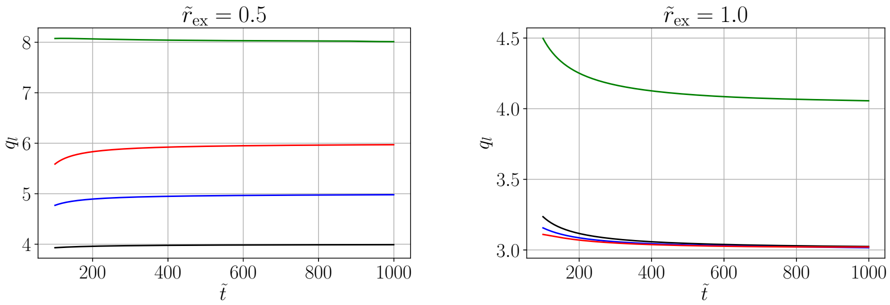

Tails: dependence on l and p

For each (n, p, l) the numerically determined decay rate q_l is shown at finite radius | at $\mathscr{I}^+$

$n = 3$	$p = 3$	$p = 4$	$p = 5$	$p = 6$	$p = 7$
$l = 0$	2|1	3|2	4|3	5|4	6|5
$l = 1$	4|2	4|2	5|3	6|4	7|5
$l = 2$	6|3	6|3	6|3	7|4	8|5
$l = 3$	8|4	8|4	8|4	8?|4	9?|5?

$n = 5$	$p = 2$	$p = 3$
$l = 0$	4|2	5?|3?
$l = 1$	6|3	6|3?
$l = 2$	8|4	8|4
$l = 3$	10|5	10?|5

Tails: dependence on l and p

Conjecture

For the NLW in $n = 3$ spatial dimensions with $p \geqslant 3$, the spherical harmonic modes in standard coordinates t, r decay as $t \to \infty$ as

$$\Phi_{lm}(t, r) \sim t^{-q_l}, \qquad q_l = \max(l + p - 1,\ 2l + 2).$$

at any fixed finite radius r.

At $\mathscr{I}^+$, the modes of the conformally rescaled scalar field $\tilde{\Phi}$ decay in hyperboloidal time $\tilde{t}$ asymptotically as

$$\tilde{\Phi}_{lm}(\tilde{t}) \sim \tilde{t}^{-\tilde{q}_l}, \qquad \tilde{q}_l = \max(p - 2,\ l + 1).$$

- Consistent with perturbative analysis [Szpak, Bizoń & Chmaj 2009] for $l = 0$ (radial symmetry) at finite radius ($\Phi \sim t^{-p+1}$).

Outline of the talk

Conclusion

- Studied focusing and defocusing, sub- and supercritical NLW in $n \geqslant 3$ spatial dimensions.
- No symmetries for $n = 3$, $\mathrm{SO}(n-1)$ symmetry for $n > 3$.
- Foliation of Minkowski spacetime into hyperboloidal slices of constant mean curvature, conformal compactification.
- Derived energy balance on hyperboloidal slices with manifestly negative flux.
- Numerical approach combines radial finite-difference with angular pseudospectral method.
- Demonstrated fourth-order convergence against exact linear solutions and self-convergence of nonlinear evolutions (energy balance, local power indices).
- Numerically determined late-time power-law decay rates (tails) for $n = 3, 5$ and various values of the nonlinearity exponent p and the spherical harmonic index l.

Outlook

- It would be interesting to try and prove the conjecture on the tail decay rates for $l > 0$ in $n = 3$ dimensions.
- A similar conjecture for higher dimensions would need more data.
- Problem: field decays very rapidly for higher exponents p. Higher than the `longdouble` precision used here (80 bits, eps $\approx 10^{-19}$) would be needed.
- Further applications of hyperboloidal code include study of singularity formation (blow-up) and threshold between blow-up and scattering.
- In radial symmetry this was studied numerically for the focusing cubic ($p = 3$) NLW in $n = 3$ [Bizoń & Zenginoğlu 2009] and in $n = 5, 7$ [Glogić, Maliborski & Schörkhuber 2020].